

Performance Evaluation of Dynamic Metasurface Antennas: Impact of Insertion Losses and Coupling

Pablo Ramírez-Espinosa*, Robin Jess Williams*, Jide Yuan* and Elisabeth de Carvalho*

*Department of Electronic Systems, Connectivity Section (CNT) Aalborg University, Denmark

Email: *{pres, rjw, jyu, edc}@es.aau.dk

Abstract—This paper evaluates the performance of multi-user massive multiple-input multiple-output (MIMO) systems in which the base station is equipped with a dynamic metasurface antenna (DMA). Due to the physical implementation of DMAs, conventional models widely-used in MIMO are no longer valid, and electromagnetic phenomena such as mutual coupling, insertion losses and reflections inside the waveguides need to be considered. Hence, starting from a recently proposed electromagnetic model for DMAs, we formulate a zero-forcing optimization problem, yielding an unconstrained objective function with known gradient. The performance is compared with that of full-digital and hybrid massive MIMO, focusing on the impact of insertion losses and mutual coupling.

Index Terms—Dynamic metasurface antennas, large intelligent surfaces, mutual coupling, mutual admittance, wireless.

I. INTRODUCTION

With the advance and popularity of metamaterials and metasurfaces, dynamic metasurface antennas (DMAs) are becoming a potential alternative to classical phased-arrays and multiple-input multiple-output (MIMO) systems [1–4]. Formally, a DMA is a collection of sub-wavelength radiating elements (e.g., complementary electric resonators [1]) deployed on top of a guiding structure, usually one-dimensional waveguides connected to a radio-frequency (RF) chain. By introducing some simple semiconductor devices into each element, the so-called reconfigurability is achieved. Stacking several of these one-dimensional structures leads to a large aperture antenna, while still keeping the necessary number of RF chains — and hence, the cost and complexity — under control.

Although very promising, the research on beamforming capabilities and transmission rate of DMAs is still in an early stage, mainly due to the lack of proper and realistic models for these structures. Compared with conventional full-digital (FD) massive MIMO (mMIMO) architectures, DMAs present several particularities that need to be considered; namely the propagation and reflections inside the waveguides, the mutual coupling between radiating element, and the dependence between the DMA configuration and the input impedance of the structure (and thus the insertion losses) [5]. These phenomena translate into two important considerations for system design: *i)* the equivalent channel depends on the specific DMA architecture (how the waveguides and elements are

deployed) and its momentaneous configuration; and *ii)* the supplied power to the DMA varies with its configuration.

Despite their relevance, the current literature consider these effects only partially when addressing the beamforming capabilities of DMAs. Some basic beamforming techniques are derived in [1], although backwards propagation in the waveguides, mutual coupling and insertion losses are ignored. More communications-oriented works are available in [4, 6], where the uplink and downlink performance is evaluated in a multiuser mMIMO system. However, only the forward propagation in the waveguides and the Lorentzian response of the elements are accounted for. The same happens with [7], where a DMA-based multiuser system is compared with full-digital and hybrid solutions. Despite the promising results, the DMA model in [7] is still oversimplified, and further studies are necessary to double check their validity in more realistic conditions.

Motivated by the lack of proper performance analyses for DMA systems, in this work we explore their beamforming capabilities when considering all the aforementioned physical phenomena. Specifically, we formulate a zero-forcing problem based on the electromagnetic model in [5] that leads to an unconstrained non-convex objective function whose gradient is provided, and compare this solution with conventional FD and hybrid mMIMO systems. In short, we try to answer two important questions: *how close is the performance of DMAs to that of mMIMO systems?*, and *what phenomena inherent to DMAs should be taken into account to render realistic results?*

Notation: Vectors and matrices are represented by bold lowercase and uppercase symbols, respectively. $(\cdot)^T$ denotes the matrix transpose, $(\cdot)^H$ is the transpose conjugate, $\|\mathbf{A}\|_F$ is the Frobenius norm, and $\|\cdot\|_2$ is the ℓ_2 norm of a vector. Also, \mathbf{I}_n is the identity matrix of size $n \times n$, $(\mathbf{A})_{j,k}$ is the j, k -th element of \mathbf{A} , and $(\mathbf{A})_{k,*}$ and $(\mathbf{A})_{*,k}$ denote the k -th row and the k -th column of \mathbf{A} respectively. Finally, $j = \sqrt{-1}$ is the imaginary number, $(\cdot)^*$ indicates complex conjugate, $\mathbb{E}[\cdot]$ is the mathematical expectation, \circ is the Hadamard product, and $\text{Re}\{\cdot\}$ and $\text{Im}\{\cdot\}$ denote real and imaginary part.

II. SYSTEM MODEL

We consider a generic mMIMO setup in which one base station (BS) serves M users simultaneously in a single cell. All the users are modeled as single-antenna devices equipped with a magnetic dipole, as discussed in the sequel, while the BS is equipped with either a FD array, digital/analog hybrid array

or DMA. Moreover, we focus on the downlink, and perfect knowledge of the channel is assumed.

For the sake of generality, the three systems are analyzed from a circuital approach, inheriting the electromagnetic model in [5]. Hence, all the actors in the system — namely transmitters, users and antennas — are represented as ports in the network. The whole network is thus described by

$$\begin{bmatrix} \mathbf{v}_t \\ \mathbf{v}_s \\ \mathbf{v}_r \end{bmatrix} = \underbrace{\begin{bmatrix} \mathbf{Y}_{tt} & \mathbf{Y}_{st}^T & \mathbf{Y}_{rt}^T \\ \mathbf{Y}_{st} & \mathbf{Y}_{ss} & \mathbf{Y}_{rs}^T \\ \mathbf{Y}_{rt} & \mathbf{Y}_{rs} & \mathbf{Y}_{rr} \end{bmatrix}}_{\mathbf{Y}} \begin{bmatrix} \mathbf{j}_t \\ \mathbf{j}_s \\ \mathbf{j}_r \end{bmatrix}, \quad (1)$$

where \mathbf{v}_k for $k \in \{t, s, r\}$ are the complex magnetic voltage vectors at the different ports (measured in amperes), \mathbf{j}_k are the magnetic current vectors (measured in volts), and the different admittance matrices $\mathbf{Y}_{k,k'}$ capture the coupling between the corresponding ports. The subindices t , s and r denote, respectively, transmitters (antennas or RF chains), DMA elements and users — see [5] for a more detailed explanation.

From (1), and applying Ohm's law at the different ports, the currents received at the users out of the reactive near-field are expressed in terms of the transmitted currents as [5, Eq. (5)]

$$\mathbf{j}_r = (\mathbf{Y}_r + \mathbf{Y}_{rr})^{-1} \left(\mathbf{Y}_{rs} (\mathbf{Y}_s + \mathbf{Y}_{ss})^{-1} \mathbf{Y}_{st} - \mathbf{Y}_{rt} \right) \mathbf{j}_t, \quad (2)$$

where $\mathbf{Y}_s \in \mathbb{C}^{L \times L}$ and $\mathbf{Y}_r \in \mathbb{C}^{M \times M}$ are diagonal matrices with elements $(\mathbf{Y}_s)_{l,l} = Y_{sl}$ and $(\mathbf{Y}_r)_{m,m} = Y_{rm}$, i.e., the load admittances at the DMA elements (if applies) and the users, respectively. Taking into account that \mathbf{j}_t is the input to the system — i.e., the output of the digital baseband precoding — we can write $\mathbf{j}_t = \mathbf{B}\mathbf{x}$, where $\mathbf{B} \in \mathbb{C}^{N \times M}$ is the precoding matrix and $\mathbf{x} \in \mathbb{C}^{M \times 1}$ is the vector of symbols intended to the M users, which is assumed to meet $\mathbb{E}[\mathbf{x}\mathbf{x}^H] = \sigma_x^2 \mathbf{I}_M$. Then, the received complex symbols are expressed as

$$\mathbf{y} = \mathbf{H}_{\text{eq}} \mathbf{B} \mathbf{x} + \mathbf{n}, \quad (3)$$

with $\mathbf{n} \sim \mathcal{CN}(\mathbf{0}, \sigma_n^2 \mathbf{I}_M)$ being the noise term and

$$\mathbf{H}_{\text{eq}} = \tilde{\mathbf{Y}}_r \left(\mathbf{Y}_{rs} (\mathbf{Y}_s + \mathbf{Y}_{ss})^{-1} \mathbf{Y}_{st} - \mathbf{Y}_{rt} \right). \quad (4)$$

where¹ $\tilde{\mathbf{Y}}_r = \sqrt{\frac{\text{Re}\{\mathbf{Y}_r\}}{2}} (\mathbf{Y}_r + \mathbf{Y}_{rr})^{-1}$.

Assuming that the channel — and thus the precoding — remains constant for a sufficiently large number of transmitted symbols², the signal-to-interference-plus-noise ratio (SINR) is expressed as

$$\gamma_m = \frac{|(\mathbf{H}_{\text{eq}})_{m,*} (\mathbf{B})_{*,m}|^2}{\frac{\sigma_x^2}{\sigma_n^2} + \sum_{k=1, k \neq m}^M |(\mathbf{H}_{\text{eq}})_{m,*} (\mathbf{B})_{*,k}|^2}, \quad (5)$$

where the transmitted power can be computed as [8]

$$P_t = \frac{1}{2} \mathbb{E} \left[\text{Re} \left\{ \mathbf{j}_t^H \mathbf{v}_t \right\} \right] = \frac{\sigma_x^2}{2} \text{Tr} \left\{ \text{Re} \left\{ \mathbf{B}^H \mathbf{Y}_p \mathbf{B} \right\} \right\}, \quad (6)$$

¹Compared to [5, Eq. (61)], we here introduce a $\sqrt{\frac{\text{Re}\{\mathbf{Y}_r\}}{2}}$ term, such that $\|\mathbf{y}\|_2^2$ equals the received power.

²This is equivalent to the widely-used block fading assumption.

where \mathbf{Y}_p is the admittance matrix at the transmitters, i.e., it is defined as $\mathbf{v}_t = \mathbf{Y}_p \mathbf{j}_t$ and naturally depends on the topology under consideration. In the following, we particularize this generic circuital model for FD mMIMO, hybrid mMIMO, and DMA systems.

A. FD and hybrid mMIMO

In this case, the ports corresponding to the DMA elements vanish in (1), and each of the transmitters directly represent one antenna attached to a dedicated RF chain, leading to the model in [9]. For the sake of coherence with the DMA case, we also model each antenna as a magnetic dipole on a perfect electric conductor (PEC) plane. Introducing $L = 0$ in (4) yields

$$\mathbf{H}_{\text{eq}}^{\text{fd}} = -\tilde{\mathbf{Y}}_r \mathbf{Y}_{rr}. \quad (7)$$

where $\mathbf{Y}_{rr} \in \mathbb{C}^{M \times M}$ represents the mutual coupling between users (diagonal matrix if they are spaced enough), and $\mathbf{Y}_{rr} \in \mathbb{C}^{M \times N}$ captures here the wireless propagation channel. Also, when backscattering is neglected, we have in this case that $\mathbf{Y}_p \approx \mathbf{Y}_{tt}$. Introducing this result in (6) renders the transmitted power for FD mMIMO systems. Also, the SINR is directly given by introducing (7) in (5). Since for every system all the antennas are modeled as magnetic dipoles, we have that the elements of \mathbf{Y}_{rr} are given by [5, Eqs. (44)-(46)]. On the other hand, in the FD system the coupling between antennas in the BS is directly given by the free space admittance (taking into account the PEC plane), i.e.,

$$(\mathbf{Y}_{tt})_{n,n'} = \begin{cases} i2\omega\epsilon G_{e2,zz}^{(a)}(\mathbf{r}_n, \mathbf{r}_{n'}) & n \neq n' \\ k\omega\epsilon/(3\pi) & n = n' \end{cases}, \quad (8)$$

with ω the angular frequency, k the wavenumber, ϵ the electrical permittivity, and $G_{e2,zz}^{(a)}(\cdot)$ as in [5, Eq. (39)].

Regarding the hybrid architecture, we here assume for simplicity a fully connected topology, which can be regarded as the upper bound in performance for hybrid mMIMO. Hence, the only difference is splitting the precoding matrix \mathbf{B} into the analog and digital matrices, i.e. the beamforming operation $\mathbf{B} = \mathbf{Q}\mathbf{R}$ is carried out in two steps: *i*) the digital precoding $\mathbf{R} \in \mathbb{C}^{S \times M}$ at the RF chains, and *ii*) the analog phase shifting at the antennas $\mathbf{Q} \in \mathbb{C}^{N \times S}$ where $|(\mathbf{Q})_{n,m}| = 1 \forall n, m$ and S is the number of RF chains.

B. DMA system model

For the DMA based system, we consider the model and topology in [5], in which the several one-dimensional waveguides are stacked and connected to dedicated RF chains, as illustrated in Fig. 1. The transmitter ports in (1) no longer represent the antennas at the BS but the output of the RF chains that feed the waveguides composing the structure. Then, the L radiating elements embedded in these waveguides are characterized by the ports carrying magnetic currents \mathbf{j}_s . The coupling between the transmitters and the radiating elements are captured in $\mathbf{Y}_{st} \in \mathbb{C}^{L \times N}$, accounting for the propagation and reflections inside the waveguides. The mutual coupling between the antenna elements (occurring both through the air and the waveguides) are described by $\mathbf{Y}_{ss} \in \mathbb{C}^{L \times L}$, and now

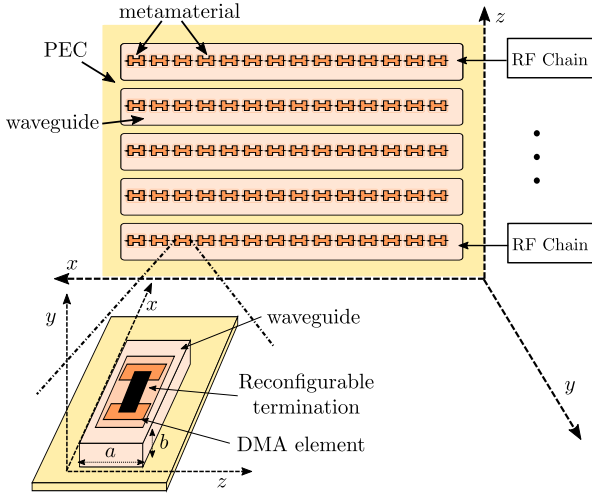


Fig. 1. Illustration of a DMA composed by one-dimensional waveguides [5].

the wireless channel is given by $\mathbf{Y}_{rs} \in \mathbb{C}^{M \times L}$ (being therefore equivalent to \mathbf{Y}_{rt} in FD and hybrid mMIMO models). Finally, $\mathbf{Y}_{rt} = \mathbf{0}$ in this case. Note that the exact expressions for all the admittance matrices are provided in [5]. Introducing these considerations in (4), the equivalent channel is given by

$$\mathbf{H}_{eq}^{dma} = \tilde{\mathbf{Y}}_r \left(\mathbf{Y}_{rs} (\mathbf{Y}_s + \mathbf{Y}_{ss})^{-1} \mathbf{Y}_{st} \right). \quad (9)$$

where, as introduced before, $\mathbf{Y}_s \in \mathbb{C}^{L \times L}$ is a diagonal matrix whose elements are the tunable load admittances of the DMA elements. The tuning is performed by adjusting the imaginary part of \mathbf{Y}_s , while the real part $\text{Re}\{(\mathbf{Y}_s)_{l,l}\} = R_s \forall l$ represents the parasitic resistance (ideally, $R_s = 0$). The transmitter admittance matrix \mathbf{Y}_p is given as

$$\mathbf{Y}_p = \mathbf{Y}_{tt} - \mathbf{Y}_{st}^T (\mathbf{Y}_s + \mathbf{Y}_{ss})^{-1} \mathbf{Y}_{st}. \quad (10)$$

Introducing (9) and (10) in (5) and (6) yields the SINR and the transmitted power for the DMA system, respectively. However, a key difference with respect to FD and hybrid mMIMO systems in terms of design is the reflection coefficient at the entry of the waveguides. Since the radiating elements of the DMA are connected serially along the feeding waveguide, the insertion losses vary with the tuning of the DMA. Therefore, the transmitted (or radiated) power is not enough to characterize the system, and the supplied power P_s is also needed, given by [5, Eq. (64)]

$$P_s = \frac{\sigma_x^2}{2} \text{Tr} \left\{ \text{Re} \left\{ \mathbf{B}^H \left(\mathbf{I}_N - \mathbf{\Gamma}^H \mathbf{\Gamma} \right)^{-1} \mathbf{Y}_p \mathbf{B} \right\} \right\}, \quad (11)$$

where $\mathbf{\Gamma} \in \mathbb{C}^{N \times N}$ is a diagonal matrix with the reflection coefficients. Ignoring the effect of the cross-waveguide coupling in the transmitter admittance, the input admittance in the waveguides is written as $\mathbf{Y}_{in} = \mathbf{Y}_p \circ \mathbf{I}_N$, rendering from [5, Eq. (9)]

$$\mathbf{\Gamma} = (\mathbf{Y}_{in} - \mathbf{I}_N Y_0) (\mathbf{Y}_{in} + \mathbf{I}_N Y_0)^{-1}, \quad (12)$$

where Y_0 is the characteristic impedance of the source and, therefore

$$P_s = \frac{\sigma_x^2}{2} \text{Tr} \left\{ \text{Re} \left\{ \mathbf{B}^H \mathbf{Y}_q \mathbf{B} \right\} \right\}, \quad \mathbf{Y}_q = \left(\mathbf{I}_N - \mathbf{\Gamma}^H \mathbf{\Gamma} \right)^{-1} \mathbf{Y}_p. \quad (13)$$

With this assumption, the reflection coefficient no longer depends on the applied precoding, being convenient for beamforming design, as shown later on. In short, it allows normalizing the transmit power through a direct scaling of the precoding matrix. Note that $P_t \leq P_s$. Since P_s represents the actual power that is consumed by the system, we use it as an optimization constraint.

III. ZERO-FORCING TRANSMIT DESIGN

A. FD and hybrid mMIMO

The zero-forcing solution for a FD mMIMO system is a well-known result given, e.g., in [10, Eq. (4.10)]. Denoting by P_t^{\max} the maximum allowed transmitted power, the constrained precoding matrix is thus written as

$$\mathbf{B}_{fd} = \frac{\sqrt{P_t^{\max}} \mathbf{H}_{fd}^\dagger}{\sqrt{\text{Tr} \left\{ \frac{\sigma_x^2}{2} (\mathbf{H}_{fd}^\dagger)^H \text{Re} \{ \mathbf{Y}_{tt} \} \mathbf{H}_{fd}^\dagger \right\}}} \quad (14)$$

with $\mathbf{H}_{fd}^\dagger = (\mathbf{H}_{eq}^{fd})^H \left(\mathbf{H}_{eq}^{fd} (\mathbf{H}_{eq}^{fd})^H \right)^{-1}$.

For the hybrid architecture, specially for the fully-connected case here considered, several works have proposed beamforming algorithms, most of them focused on approximating the optimal precoding matrix by accounting for the modulus constraint in the phase shift matrix [11–13]. In our case, we rely on the recently proposed optimal zero-forcing precoder in [13], summarized here in **Algorithm 1** for the reader's convenience, where s is the chosen step size for gradient descent and the different matrices involved are computed as

$$\begin{aligned} \mathbf{C}_h &= \left(\mathbf{R}^H \mathbf{R} \right)^{-1} \mathbf{R}^H \left(\mathbf{H}_{eq}^{fd} \right)^H, \quad \mathbf{Q} = e^{i\Theta}, \\ \mathbf{A}_h &= \left(\mathbf{H}_{eq}^{fd} \mathbf{R} \mathbf{C}_h \right)^{-1}, \quad \mathbf{V} = (\mathbf{C}_h \mathbf{A}_h)^H, \\ \mathbf{U} &= \left(\mathbf{R} \mathbf{C}_h - \left(\mathbf{H}_{eq}^{fd} \right)^H \right) \mathbf{A}_h. \end{aligned} \quad (15)$$

B. DMA zero-forcing beamforming

Starting from the general communication model in (3), we can cancel the inter-user interference by following the same approach as in FD systems in (14), setting therefore the baseband precoding matrix to

$$\mathbf{B}_{dma} = \frac{\sqrt{P_t^{\max}} \mathbf{H}_{dma}^\dagger}{\sqrt{\text{Tr} \left\{ \frac{\sigma_x^2}{2} (\mathbf{H}_{dma}^\dagger)^H \text{Re} \{ \mathbf{Y}_q \} \mathbf{H}_{dma}^\dagger \right\}}} \quad (16)$$

where \mathbf{H}_{dma}^\dagger is the pseudo-inverse of the DMA equivalent channel in (9), i.e.,

$$\mathbf{H}_{dma}^\dagger = (\mathbf{H}_{eq}^{dma})^H \left(\mathbf{H}_{eq}^{dma} (\mathbf{H}_{eq}^{dma})^H \right)^{-1}. \quad (17)$$

Algorithm 1: Hybrid Zero-Forcing [13]

1 **Input:** $\mathbf{H}_{\text{eq}}^{\text{fd}}, P_t^{\text{max}}, \mathbf{Y}_{\text{tt}}, s$;
2 **Initialization:** random $\Theta \in \mathbb{R}^{N \times L}$;
3 **while not converge do**
4 Compute RF precoder \mathbf{Q} and auxiliary matrices \mathbf{C}_h ,
 \mathbf{A}_h , \mathbf{U} , and \mathbf{V} by (15);
5 Compute objective gradient $f(\mathbf{Q}) =$
 $2 \operatorname{Im} \left\{ \left[\mathbf{U} \left(\mathbf{A}_h \circ \mathbf{I}_N - \frac{N}{\frac{P_t^{\text{max}}}{\sigma_x^2} + \operatorname{Tr}\{\mathbf{A}_h\}} \mathbf{I}_N \right) \mathbf{V} \right] \circ \mathbf{Q}^* \right\}$
 ;
6 Update $\Theta = \Theta - s f(\mathbf{Q})$;
7 **end**
8 Compute $\mathbf{O} = \mathbf{C}\mathbf{A}$;
9 Compute diagonal power allocation matrix \mathbf{P} , where
 $(\mathbf{P})_{n,n} = \sqrt{\frac{P_t^{\text{max}} + \operatorname{Tr}\{\mathbf{A}_h\} \sigma_n^2}{M(\mathbf{A}_h)_{n,n} - \sigma_n^2}}$;
10 Compute $\mathbf{R} = \frac{P_t^{\text{max}} \mathbf{O} \mathbf{P}}{\sqrt{\operatorname{Tr}\left\{ \frac{\sigma_x^2}{2} (\mathbf{Q} \mathbf{O} \mathbf{P})^H \operatorname{Re}\{\mathbf{Y}_{\text{tt}}\} \mathbf{Q} \mathbf{O} \mathbf{P} \right\}}}$;
11 **Outputs:** \mathbf{Q}, \mathbf{R}

Note that we are considering \mathbf{Y}_q in (13) and, hence, the supplied power instead of the transmitted power, allowing for insertion losses control. Introducing now (16) in (5), we have that

$$\gamma_m = \gamma = \frac{P_t^{\text{max}} \sigma_x^2}{\sigma_n^2 \operatorname{Tr} \left\{ \frac{\sigma_x^2}{2} (\mathbf{H}_{\text{dma}}^\dagger)^H \operatorname{Re}\{\mathbf{Y}_q\} \mathbf{H}_{\text{dma}}^\dagger \right\}}, \quad \forall m \quad (18)$$

where, as expected, the signal-to-noise ratio (SNR) is the same for all the users (under the very mild assumption of similar noise power at each user). The beamforming problem is therefore formulated as

$$\mathcal{P1} \text{ (ZF)}: \underset{\mathbf{Y}_s}{\text{maximize}} \quad \gamma \quad (19a)$$

$$\text{s.t. } \operatorname{Re}\{(\mathbf{Y}_s)_{i,i}\} = R_s \quad \forall i. \quad (19b)$$

As defined in Section II-B, \mathbf{Y}_s is a diagonal matrix with the load admittance of each DMA element, and whose real part R_s represents the losses. Then, constraint (19b) can be easily removed by defining $\mathbf{Y}_s^{\text{im}} \in \mathbb{R}^{L \times L}$ such that $\mathbf{Y}_s^{\text{im}} = \operatorname{Im}\{\mathbf{Y}_s\}$ and $\tilde{\mathbf{Y}}_{\text{ss}} = R_s \mathbf{I}_L + \mathbf{Y}_{\text{ss}}$. Hence, we can now optimize over the real matrix \mathbf{Y}_s^{im} while incorporating the losses of the elements in \mathbf{Y}_{ss} . Moreover, for the sake of notation, we define $\tilde{\mathbf{Y}}_{\text{rs}} = \tilde{\mathbf{Y}}_{\text{r}} \mathbf{Y}_{\text{rs}}$, so the DMA equivalent channel reads

$$\mathbf{H}_{\text{eq}}^{\text{dma}} = \tilde{\mathbf{Y}}_{\text{rs}} \left(j \mathbf{Y}_s^{\text{im}} + \tilde{\mathbf{Y}}_{\text{ss}} \right)^{-1} \mathbf{Y}_{\text{st}}. \quad (20)$$

With the above definitions, the optimization problem in (19) is finally simplified to

$$\mathcal{P2} \text{ (ZF)}: \underset{\mathbf{Y}_s^{\text{im}}}{\text{minimize}} \quad f(\mathbf{Y}_s^{\text{im}}) \quad (21)$$

$$f(\mathbf{Y}_s^{\text{im}}) = \operatorname{Tr} \left\{ \operatorname{Re}\{\mathbf{Y}_q\} \mathbf{H}_{\text{dma}}^\dagger (\mathbf{H}_{\text{dma}}^\dagger)^H \right\}. \quad (22)$$

Problem $\mathcal{P2}$ is unconstrained and, in general, non-convex. The difficulty lies on the inverse term $\left(j \mathbf{Y}_s^{\text{im}} + \tilde{\mathbf{Y}}_{\text{ss}} \right)^{-1}$, that appears several times in both \mathbf{Y}_q and $\mathbf{H}_{\text{dma}}^\dagger$. However, since the problem is unconstrained, approximated solutions can be found by using conventional optimization algorithms available in the literature. In our case, we rely on trust-region methods [14], which approximate the objective by a quadratic function in a *trusted region*, i.e., a region where the expected ratio between the expected improvement and the true one is similar. Trust-region optimization is available in standard calculation software such as MATLAB, being therefore convenient. Specifically, we use *fminunc* function from MATLAB, which implements a simplified trust-region algorithm proposed in [15]. The requirement of this algorithm is providing the gradient of the objective function $f(\mathbf{Y}_s^{\text{im}})$, which can be written in closed-form as in (26) at the top of next page, with the involved auxiliary matrices as

$$\mathbf{A}^{-1} = (j \mathbf{Y}_s^{\text{im}} + \tilde{\mathbf{Y}}_{\text{ss}})^{-1}, \quad (23)$$

$$\mathbf{C} = ((\mathbf{Y}_p + \mathbf{Y}_0) \circ \mathbf{I}_N)^{-1}, \quad (24)$$

$$\mathbf{D} = (\mathbf{I}_N - \mathbf{\Gamma}^H \mathbf{\Gamma})^{-1}. \quad (25)$$

Due to space constraints, the proof is omitted here, but (26) is obtained by following standard complex matrix differentiation techniques [16]. Note also that, since \mathbf{Y}_s^{im} is a diagonal matrix, only the diagonal elements of (26) are necessary.

Naturally, the here proposed solution to $\mathcal{P2}$ is not suitable for real-time implementation, and simpler —albeit suboptimal— algorithms are necessary. However, the trust-region solver with (26) is indeed suitable for performance analysis, providing a reasonable idea on what can be expected from DMA based systems.

IV. PERFORMANCE EVALUATION

To compare the performance of the three systems, we run in this section a thorough set of Monte Carlo simulations over correlated Rayleigh channel. Specifically, the channel to the m th user is given as $\mathbf{f}_m \sim \mathcal{CN}(\mathbf{0}, \delta \Sigma)$ for all $m = 1, \dots, M$. Resuming the circuital models presented in Section II, for the FD and hybrid mMIMO systems we have $(\mathbf{Y}_{\text{tt}})_{m,*} = \mathbf{f}_m^T$, and for the DMA system $(\mathbf{Y}_{\text{rs}})_{m,*} = \mathbf{f}_m^T$.

The entries of the co-variance matrix Σ are normalized such that a FD system with a single antenna, a conjugate load admittance $Y_{\text{rm}} = Y_{\text{rt}}^*$, and $\sigma_x^2 = 1$ achieves a SNR of δ , being therefore the reference system. Hence, using Eqs. (3), (6), and (7), we can write the following relation

$$\mathbb{E} \left[\frac{P_r}{P_t} \right] = \mathbb{E} \left[\frac{|H_{\text{eq}}^{\text{fd}} B x|^2}{\frac{1}{2} \operatorname{Re}\{x^H B^H Y_{\text{tt}} B x\}} \right] = \frac{9 \delta \sigma_y^2 \pi^2}{2 k^2 \omega^2 \epsilon^2}, \quad (27)$$

where $\delta \sigma_y^2$ is the variance of the channel Y_{rt} and (8) and [5, Eq. (46)] have been applied. Dividing by the noise variance yields the nominal SNR as

$$\bar{\gamma} = \delta \frac{\sigma_y^2}{\sigma_n^2} \frac{9 \pi^2}{2 k^2 \omega^2 \epsilon^2} \implies \sigma_y^2 = \frac{2 k^2 \omega^2 \epsilon^2 \sigma_n^2}{9 \pi^2}, \quad (28)$$

$$\begin{aligned}
\frac{\partial f(\mathbf{Y}_s^{\text{im}})}{\partial \mathbf{Y}_s^{\text{im}}} = & \text{Im} \left\{ \left(\mathbf{A}^{-H} \mathbf{Y}_{\text{st}}^* \left[\left((\mathbf{I}_N - \mathbf{\Gamma}^H) \mathbf{\Gamma} \mathbf{Y}_q \mathbf{H}_{\text{dma}}^\dagger (\mathbf{H}_{\text{dma}}^\dagger)^H \mathbf{D} \mathbf{C}^H \right) \circ \mathbf{I}_N \right] \mathbf{Y}_{\text{st}}^H \mathbf{A}^{-H} \right) \right\} \\
& - \text{Im} \left\{ \left(\mathbf{A}^{-1} \mathbf{Y}_{\text{st}} \left[\left(\mathbf{C} \mathbf{Y}_q \mathbf{H}_{\text{dma}}^\dagger (\mathbf{H}_{\text{dma}}^\dagger)^H \mathbf{D} \mathbf{\Gamma}^H (\mathbf{I}_N - \mathbf{\Gamma}) + \mathbf{H}_{\text{dma}}^\dagger (\mathbf{H}_{\text{dma}}^\dagger)^H \mathbf{D} \right) \circ \mathbf{I}_N \right] \mathbf{Y}_{\text{st}}^T \mathbf{A}^{-1} \right) \right\} \\
& - 2 \text{Im} \left\{ \left(\mathbf{A}^{-1} \mathbf{Y}_{\text{st}} \left[\mathbf{H}_{\text{dma}}^\dagger (\mathbf{H}_{\text{dma}}^\dagger)^H \text{Re}\{\mathbf{Y}_q\} - (\mathbf{I}_N - \mathbf{H}_{\text{dma}}^\dagger \mathbf{H}_{\text{eq}}^{\text{dma}}) \text{Re}\{\mathbf{Y}_q\} \mathbf{H}_{\text{dma}}^\dagger (\mathbf{H}_{\text{dma}}^\dagger)^H \right] \mathbf{H}_{\text{dma}}^\dagger \tilde{\mathbf{Y}}_{\text{rs}} \mathbf{A}^{-1} \right) \right\}. \quad (26)
\end{aligned}$$

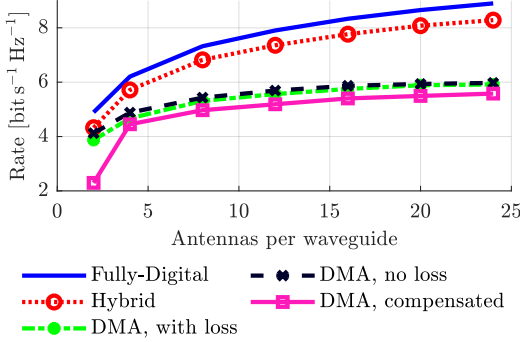


Fig. 2. Simulated per user rate for the three presented topologies. There are $M = 5$ users being served by $N = 6$ RF chains in the hybrid and DMA systems, and the number of antennas connected to each RF chain is increased according to the x axis. For the FD system, the number of RF chains is N times the number of antennas per waveguide. The spacing between the elements is set to 0.5λ , the spacing between waveguides is λ .

such that $\bar{\gamma} = \delta$. Hence, using the covariance matrix in [5, Eq. (59)] with $\sigma_\alpha^2 = \frac{2k^2\omega^2\epsilon^2\sigma_n^2}{9\pi^2} \frac{3}{4\pi}$, and generating the channels using $\mathbf{f}_m \sim \mathcal{CN}(\mathbf{0}, \delta\mathbf{\Sigma})$, the nominal SNR is given directly by δ . Therefore, in the following simulations the channel power is scaled according to that reference and kept constant for all the systems so that $\bar{\gamma} = 13\text{dB}$. Also, the frequency is set to $f = 10\text{GHz}$, the width and height of the DMA waveguides are, respectively, $a = 0.73\lambda$ and $b = 0.167\lambda$, with λ being the wavelength, and the intrinsic admittance at the entrance of the waveguides is $Y_0 = 35.33\text{S}$.

The first numerical result is depicted in Fig. 2, where the impact of the insertion losses in the DMA system is evaluated. Specifically, for the DMA we consider $N = 6$ RF chains, and start increasing the number of elements per waveguide to see the impact in performance. Three different curves are shown for the DMA: *i*) the result obtained for the algorithm in Section III (labeled as “DMA with loss”), *ii*) the performance given by the same algorithm when the reflection coefficient is ignored in the optimization — we set $\mathbf{\Gamma} = \mathbf{0}$ in (26) — (labeled as “DMA, no loss”), and *iii*) the same as before, but the transmitted power is re-scaled so that the supplied power is below P_t^{max} (labeled as “DMA compensated”).

The performance of the DMA system is compared with the hybrid topology with the same number of RF chains and

antennas, and with the FD system when the number of antennas is equal to that in the other systems. Regarding Fig. 2, the first aspect we notice is that, as expected, the FD system renders the best performance, but at the cost of a much larger number of RF chains. Secondly, we observe that the hybrid solution provides a decent performance while keeping under control the number of RF chains; however, note we are using a fully-connected layout, and therefore the required number of phase shifters (and the potential cost) is still high. As for the DMA systems, we see that the performance when the insertion losses are considered (green curve) is almost identical to the case without losses (black curve), showing that we can actually control the reflection coefficient in the proposed algorithm. We see, in turn, a drop in performance when the insertion losses are neglected, although the gap seems to reduce as the waveguides are more populated.

Another interesting observation is that the DMA system seems to have an upper bound in the achievable rate, in contrast to the FD and hybrid mMIMO topologies. This is coherent with how a DMA works. The power introduced in the waveguides is in part radiated by the first element (according to the termination admittance), and the remaining power keeps propagating until reaching the next element, where the procedure repeats. It is intuitive then that, as we increase the number of elements, less and less power reaches the final elements. One may think that the same happens in FD and hybrid systems, but in those topologies, the amplitude and the phase shift induced in the antennas are independent, therefore the power can be equally split between antennas (if this would be necessary). However, in a DMA, the amount of power that you radiate by an element and the induced phase shift are related, as explained [5]. Hence, this leads to the conclusion that may be an optimal number of elements per waveguide in terms of cost and performance ratio.

Motivated by the gap in performance between FD and hybrid systems and the DMA, we explore in Fig. 3 how many elements we need to match the performance of a FD system. More specifically, we consider a rectangular array in the FD case, with 6 rows and varying number of columns spaced 5λ , increasing thus the number of total antennas. For each number of columns, we explore the number of required antennas in both hybrid and DMA systems (denoted by L) with $N = 6$ RF chains. The aperture of the array is kept constant, so to increase the

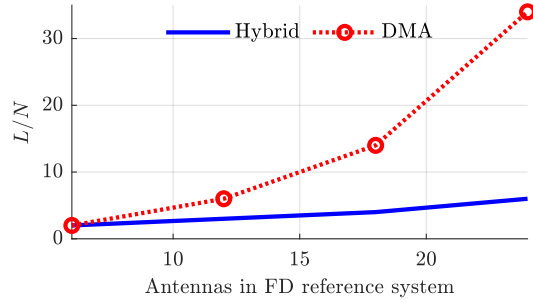


Fig. 3. Number of required antennas in hybrid mMIMO and DMA systems to match the performance of a FD array with varying number of antennas.

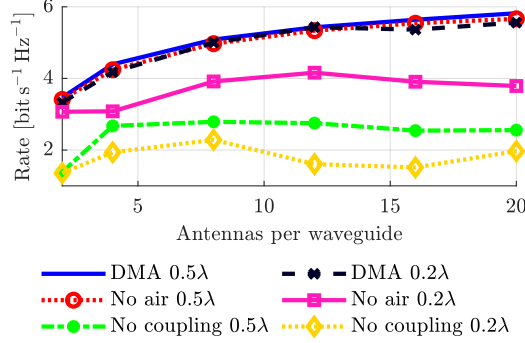


Fig. 4. Impact of mutual coupling in simulated per user rate for the DMA system. There are $M = 4$ users being served by $N = 4$ RF with different number of elements. The spacing between the elements is set to 0.5λ , the spacing between waveguides is λ .

number of elements we reduce the spacing between them. As observed from Fig. 3, while the number of antennas attached to each RF chain in hybrid systems seemingly increases linearly, it does exponentially for the DMA. This is coherent with the upper bound in performance observed before.

Finally, we evaluate the impact of mutual coupling in the beamforming solution. To that end, we compare the performance of the proposed zero-forcing algorithm in the following cases: *i*) the DMA system as described in Section II (labelled as “DMA”), *ii*) the case where the coupling through the air between the elements is ignored³ (labelled as “No air”) and *iii*) the mutual coupling is completely ignored, i.e., \mathbf{Y}_{ss} is enforced to be diagonal (labelled as “No coupling”).

The performance of the aforementioned cases is shown in Fig. 4 for two different spacing values between elements: 0.5λ and 0.2λ . Judging from the results, we clearly see that completely ignoring the coupling leads to a considerably worse performance, while ignoring the coupling through the air is only a reasonable approximation when the spacing between the elements is large. These conclusions are coherent and intuitive, and highlight the necessity of properly modeling the mutual coupling — both through air and waveguides — in DMA based systems.

³The value of $G_{e2,zz}^{(a)}$ when computing [5, Eq. (37)] is neglected.

V. CONCLUSIONS

We have provided a complete and electromagnetic-compliant performance evaluation of DMA based systems when a zero-forcing beamforming is applied. The results show that, in contrast to mMIMO systems, DMAs have an upper bound in the achievable rate, and adding more elements per waveguide does not lead to a performance increase once a certain threshold is reached. Also, it has been shown that insertion losses should be considered in the optimization, and that the impact of mutual coupling — specially that through the waveguides — is highly relevant. These conclusions are in striking contrast to those observed in other works available in the literature, highlighting the importance of a good modeling when analyzing what can be expected from real systems.

REFERENCES

- [1] D. R. Smith, O. Yurduseven, L. P. Mancera, P. Bowen, and N. B. Kundtz, “Analysis of a waveguide-fed metasurface antenna,” *Phys. Rev. Applied*, vol. 8, p. 054048, Nov 2017.
- [2] T. Sleasman, M. F. Imani, W. Xu, J. Hunt, T. Driscoll, M. S. Reynolds, and D. R. Smith, “Waveguide-fed tunable metamaterial element for dynamic apertures,” *IEEE Antennas Wireless Propag. Lett.*, vol. 15, pp. 606–609, 2016.
- [3] N. Shlezinger, G. C. Alexandropoulos, M. F. Imani, Y. C. Eldar, and D. R. Smith, “Dynamic metasurface antennas for 6G extreme massive MIMO communications,” *IEEE Wireless Commun.*, vol. 28, no. 2, pp. 106–113, 2021.
- [4] N. Shlezinger, O. Dicker, Y. C. Eldar, I. Yoo, M. F. Imani, and D. R. Smith, “Dynamic metasurface antennas for uplink massive mimo systems,” *IEEE Trans. Commun.*, vol. 67, no. 10, pp. 6829–6843, 2019.
- [5] R. J. Williams, P. Ramírez-Espinosa, J. Yuan, and E. De Carvalho, “Electromagnetic based communication model for dynamic metasurface antennas,” *IEEE Trans. Wireless Commun. (Early Access)*, pp. 1–1, 2022.
- [6] H. Wang, N. Shlezinger, S. Jin, Y. C. Eldar, I. Yoo, M. F. Imani, and D. R. Smith, “Dynamic metasurface antennas based downlink massive MIMO systems,” in *IEEE 20th Int. Workshop Signal Process. Adv. Wireless Commun. (SPAWC)*, 2019, pp. 1–5.
- [7] H. Zhang, N. Shlezinger, F. Guidi, D. Dardari, M. F. Imani, and Y. C. Eldar, “Beam focusing for near-field multi-user MIMO communications,” *arXiv preprint arXiv:2105.13087 [eess.SP]*, 2021.
- [8] D. M. Pozar, *Microwave engineering*, 4th ed. Hoboken, NJ: Wiley, 2012, oCLC: ocn714728044.
- [9] R. Jess Williams, P. Ramírez-Espinosa, E. de Carvalho, and T. L. Marzetta, “Multiuser MIMO with large intelligent surfaces: Communication model and transmit design,” in *ICC 2021 - IEEE Int. Conf. Commun.*, 2021, pp. 1–6.
- [10] E. Björnson, J. Hoydis, and L. Sanguinetti, *Massive MIMO Networks: Spectral, Energy, and Hardware Efficiency*, 2017.
- [11] X. Yu, J.-C. Shen, J. Zhang, and K. B. Letaief, “Alternating minimization algorithms for hybrid precoding in millimeter wave MIMO systems,” *IEEE J. Sel. Topics Signal Process.*, vol. 10, no. 3, pp. 485–500, 2016.
- [12] S. S. Ioushua and Y. C. Eldar, “A family of hybrid analog–digital beamforming methods for massive MIMO systems,” *IEEE Trans. Signal Process.*, vol. 67, no. 12, pp. 3243–3257, 2019.
- [13] X. Su and Y. Jiang, “Optimal Zero-Forcing Hybrid Downlink Precoding for Sum-Rate Maximization,” *IEEE Wireless Communications Letters*, vol. 11, no. 3, pp. 463–467, Mar. 2022. [Online]. Available: <https://ieeexplore.ieee.org/document/9634170/>
- [14] A. R. Conn, N. I. M. Gould, and P. L. Toint, *Trust-Region Methods*. USA: Society for Industrial and Applied Mathematics, 2000.
- [15] R. H. Byrd, R. B. Schnabel, and G. A. Shultz, “Approximate solution of the trust region problem by minimization over two-dimensional subspaces,” *Mathematical programming*, vol. 40, no. 1, pp. 247–263, 1988.
- [16] A. Hjørungnes, *Complex-Valued Matrix Derivatives: With Applications in Signal Processing and Communications*, 1st ed. USA: Cambridge University Press, 2011.